ground water

Permeability Hysterisis of Limestone During Isotropic Compression

by A.P.S. Selvadurai[1] and A. Głowacki[2]

Abstract

The evolution of permeability hysterisis in Indiana Limestone during application of isotropic confining pressures up to 60 MPa was measured by conducting one-dimensional constant flow rate tests. These tests were carried out either during monotonic application of the confining pressure or during loading-partial unloading cycles. Irreversible permeability changes occurred during both monotonic and repeated incremental compression of the limestone. Mathematical relationships are developed for describing the evolution of path-dependent permeability during isotropic compression.

Introduction

In conventional geosciences such as hydrogeology, ground water flow, and geotechnical engineering, the bulk permeability of a geomaterial is generally considered to be a sessile property. Permeability of geomaterials can evolve due to external actions such as mechanical and thermal loading. Pore fabric alterations by dissolution and precipitation of minerals during advective transport of reactive chemicals within the pore space and molecular diffusion within the impervious grain structure can also lead to permeability alterations. These phenomena are important for the deep geological disposal and storage of hazardous nuclear fuel wastes and other contaminants, oil and gas extraction and storage, and the modeling of the mechanics of active geological faults. We examine here the alteration in the permeability of competent geological materials resulting from changes to an ambient isotropic stress field; examples include deep mines and other openings located at significant depths below the earth's surface. In these cases, the alteration in the near-field stress state due to stress release can induce changes in both the mechanical and fluid transport characteristics. In general, the alteration in the in situ stress state due to the creation of a deeply located opening is three-dimensional and can contribute to a variety of phenomena, including brittle fracture, rock bursts, yielding of the rock, and development of micromechanical continuum damage in the form of microcrack and microvoid evolution. The influence of these processes on the mechanical and transport characteristics are, however, specific for each geological material. Investigations of the stress state–induced evolution of both mechanical and fluid transport phenomena are rare because of the coupling between the mechanical and flow processes and the stress path dependency of the alteration process. It is difficult to perform fluid transport experiments when the geological sample is subjected to anisotropic stress states. The application of true triaxial stress states, which include homogeneous tensile stress states, is difficult to realize under routine experimentation. Early research on the alteration of fluid transport characteristics due to confining stresses was done by Fatt and Davis (1952) and Fatt (1953), who investigated the reduction in permeability due to overburden effects. McLatchie et al. (1958) discussed the influence of compressibility on the permeability of reservoir rock, noting the correlation between permeability reduction both with confining stresses and with an increase in the observed clay content. Wyble (1958) and Gray (1962) showed a reduction in the permeability and porosity of anisotropic sandstone during isotropic compression. The radial percolation test (Londe and Sabarly

[1]Corresponding author: Corresponding author: Department of Civil Engineering and Applied Mechanics, McGill University, 817 Sherbrooke Street West, Montreal, Quebec, Canada H3A 2K6; (514) 398-6672; fax (514) 398-7361; patrick.selvadurai@mcgill.ca

[2]Department of Civil Engineering and Applied Mechanics, McGill University, 817 Sherbrooke Street West, Montreal, Quebec, Canada H3A 2K6.

Received May 2007, accepted September 2007.

doi: 10.1111/j.1745-6584.2007.00390.x

1966; Jaeger 1972) involves subjecting a cylindrical sample of saturated rock containing a cylindrical cavity to an external radial stress field; in Jaeger's (1972) radial percolation tests, the converging radial flow occurs into a partially penetrating central cavity. The skeletal stress state induced by the external pressurization of a partially penetrating central cavity in a cylinder is complex, leading to an uncertainty in the interpretation of the evolution of permeability with confining pressure. The intergranular stresses within a porous rock can have a considerable influence on its permeability: Large stress fields such as those found at significant depths within the earth or within the core of a concrete dam can cause deformation of the pore skeleton and induce closure and/or collapse of the pathways, contributing to permeability of the porous medium. Knutson and Bohor (1963) assessed the reduction of permeability of Miocene sandstone and unconsolidated sand when subjected to confining pressures up to 100 MPa, indicating that irreversible alterations in the pore structure lead to irreversible permeability changes. Brace et al. (1968) subjected Westerly granite samples to confining pressures as large as 400 MPa, observing permeability reductions from 3.5×10^{-19} m^2 at 5 MPa to 3.9×10^{-21} m^2 at 400 MPa, a trend also observed by Bernaix (1966), Kranz et al. (1979), and Wright et al. (2002). Experiments by Lion et al. (2004a, 2004b) on Oolitic limestone saturated with ethanol showed a permeability decrease with increasing confining pressure, while mineralogical and microscopic analysis did not reveal any crack closure under hydrostatic loading. Heystee and Roegiers (1981), however, noted increases in the permeability of rock specimens subjected to tensile stresses. References to further studies are given in Lama and Vutukuri (1978), Selvadurai and Carnaffan (1997), and Selvadurai et al. (2005). Several investigators have assessed permeability changes in a variety of materials due to damage evolution, in the form of microcrack generation and void nucleation, under triaxial stress states. Results of Zoback and Byerlee (1975) on granite showed increases of up to a factor of four in the magnitude of the permeability, while Shiping et al. (1994) showed that in sandstone, all combinations of stress states employed in their tests produced an increase in permeability. Triaxial test results on anisotropic granite (Kiyama et al. 1996) also indicated increases in the permeability characteristics. Zhu and Wong (1997) suggested void collapse-associated reductions in the permeability of Berea Sandstone; at confining stresses in the range of 10 MPa and at a peak deviator stress of 100 MPa, the permeability remained unchanged. At higher confining stresses of the order of 250 MPa and peak deviator stresses in the same range, the permeability reduced from 10^{-13} to 10^{-16} m^2, but there is no record of whether this permeability evolution is irreversible. Tests conducted on rocks and clay by Coste et al. (2001) concluded that there was an increase in permeability, up to 2 orders of magnitude, with an increase in deviatoric stresses. The literature on stress-induced changes in the permeability of rocks is limited; Selvadurai (2004) provides a review of experimental investigations that indicate enhancement of permeability of geomaterials with triaxial stress states. In contrast, there are many investigations of the mechanical behavior of rocks under high pressure (e.g., Shimada 2000).

This research examines the reduction and the accompanying hysterisis in the permeability of Indiana Limestone subjected to isotropic compressive stresses up to 60 MPa. The experiments were conducted on jacketed cylindrical samples of the limestone measuring approximately 100 mm in diameter and 200 mm in height, and approximate relationships are proposed to describe the isotropic stress state–dependent evolution of the permeability characteristics. Although there are several techniques that could be used, including the transient and oscillating pressure pulse techniques (Suri et al. 1997; Selvadurai et al. 2005) and the Standard Test Method for Measuring Permeability of Rock by Flowing Air (ASTM Standard D4525), the steady-state flow test is the most straightforward and is less dependent on the mechanical and physical properties of both the porous medium and the permeating fluid.

The Test Facility and Experimental Procedure

Figure 1a presents a cross section of the triaxial cell capable of subjecting soil and rock samples to cell pressures up to 65 MPa and axial loads up to 250 kN. The cell pressure is supplied using a digitally controlled servohydraulic system, with all components pressure rated for 83 MPa. The test samples are mounted on a pedestal of diameter 100 mm, located on the base unit of the triaxial cell; this base pedestal has two entry ports to provide water flow to the sample, and the sample is sealed by a stainless steel plate. In this arrangement, the sample can be subjected to cell pressure as well as to flow through the sample at a known hydraulic gradient. The interface between the end plates and the sample contains geotextile layers with an undeformed thickness of approximately 2 mm. At peak confining pressures in the range of 65 MPa, the geotextile experiences significant compression with a reduction in its permeability characteristics. The reduced permeability is, however, significantly higher (2.3×10^{-7} m^2) than the permeability of the Indiana Limestone; when estimating the permeability of the limestone, the permeability of both the geotextile and the system was accounted for. The typical sample assembly (without a confining membrane) on the base pedestal of the triaxial apparatus is shown in Figure 1b. The membrane used to seal the sample should be capable of withstanding the applied peak cell pressures without rupture through contact with either the surface of the limestone or the geotextile layers. The chosen membrane was a close-fitting nitrile rubber membrane of thickness 2 mm with an unstretched internal diameter of 91 mm. Flow through the pressurized limestone sample was delivered at flow rates as low as 0.10 mL/min. The pressure induced during the attainment of a steady flow rate was monitored using a pressure transducer attached to the water supply line. Both the cell pressure and the fluid pressure were monitored throughout the test.

One-dimensional flow was induced in a jacketed cylindrical sample of the Indiana Limestone, with impervious contact between the cylindrical surface of the limestone and the jacketing membrane (Figure 1c). In order

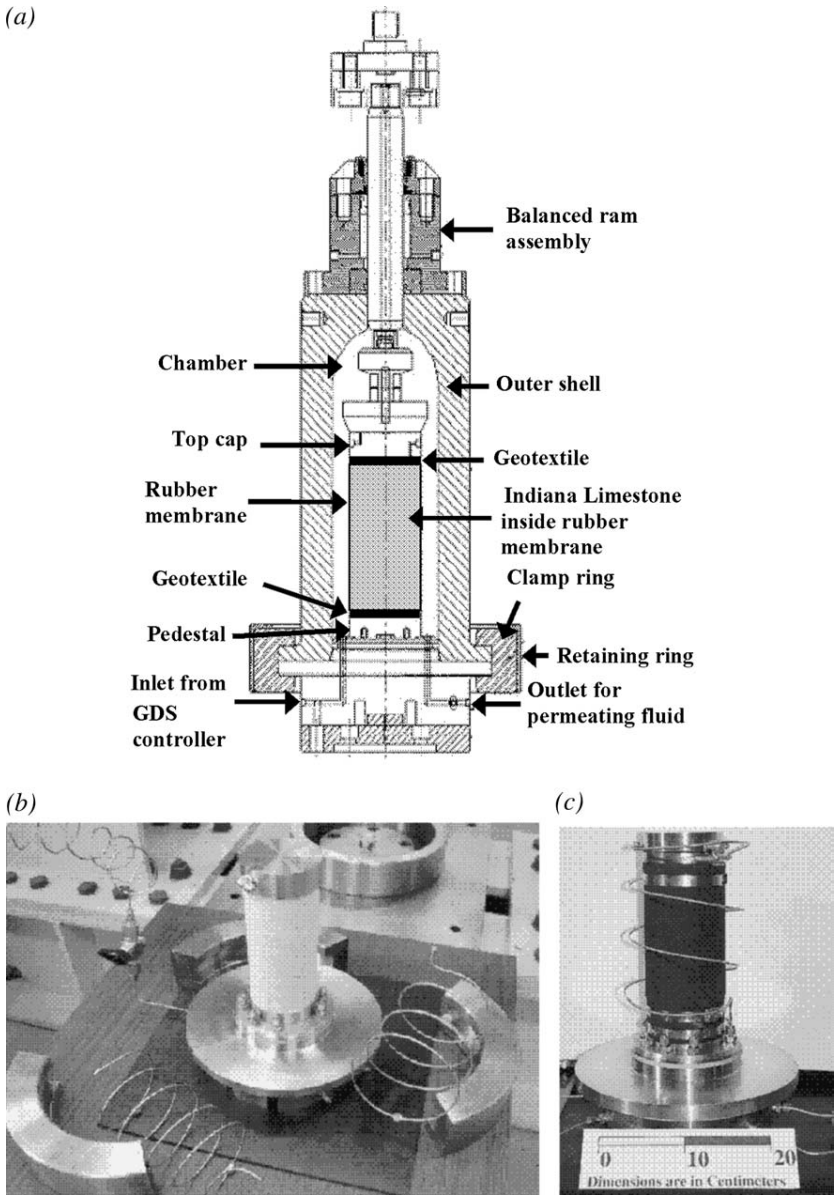

Figure 1. Cross section of the high-pressure triaxial cell and assembly views of the sample setup.

to accurately interpret the flow rate through the limestone, the same nominal confining stress was applied to each jacketed sample. Information on the mineralogical composition of the limestone was provided by the supplier and is also available in a number of other investigations of Indiana Limestone (e.g., ILIA 1998). Core samples of the limestone measuring 108 mm in diameter and 200 mm in length were machined to a diameter of 100 mm, resulting in a relatively smooth external surface. The irregular surfaces of the ends of the limestone cylinders were polished to achieve a roughness similar to that of the cylindrical surface. Eleven samples were recovered from the limestone block and were used for the permeability tests and companion research programs to evaluate the permeability of the limestone under unstressed conditions and to determine the mechanical and physical properties of the rock, including the elastic constants and porosity. In its as-supplied condition, the Indiana Limestone used in this investigation had the following mechanical and physical properties: Young's modulus almost equal to 24 GPa, Poisson's ratio almost equal to 0.14, bulk unit weight almost equal to 22 kN/m^3, and porosity almost equal to 0.17.

The limestone sample was vacuum saturated for 48 h prior to placing it in the jacketing membrane. The jacketed sample was installed on the lower pedestal of the apparatus, with geotextile discs on the upper and lower ends, and subjected to a secondary saturation period of 48 h at a flow rate of 1 mL/min in order to observe the integrity of the membrane and the seals. The outer shell of the triaxial apparatus was then assembled and the chamber filled with distilled water, keeping the inlet and outlet ports closed to minimize any desaturation of the limestone sample (Figure 2). Ideally, during high-pressure testing, the pressurizing fluid should be an incompressible mineral oil such as silicone oil. In the

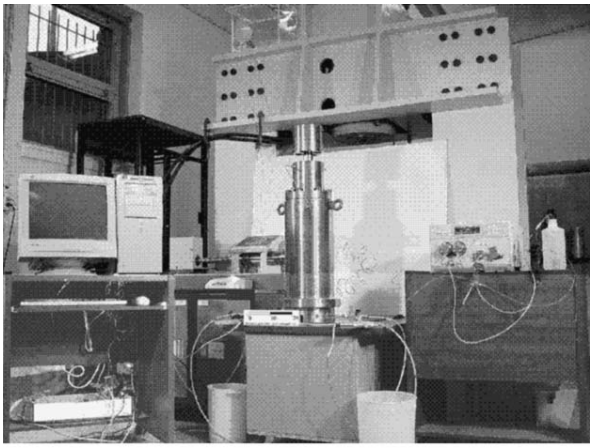

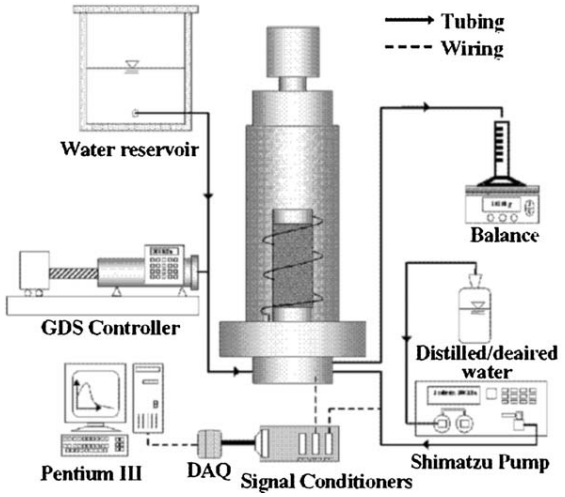

Figure 2. General and schematic views of the experimental facility.

present set of experiments, water was used as the pressurizing fluid. Prior to the application of the confining pressures, the entire system, including the tubing and the connections, was primed by setting the Geotechnical Digital Systems (GDS) controller to 250 kPa; this allowed the entire system to be pressurized, facilitating the release of any trapped air. In the test sequence, the cell pressure was applied and the system allowed to attain equilibrium as evidenced by the development of stable cell pressures over a 15-min period. Deaired distilled water was then pumped through the sample at a specified rate of 1 mL/min for 1 h to establish a steady flow rate. Since the specimen was subjected to a high cell pressure over a prolonged period, it was necessary to check for relaxation of the system, which could affect the cell pressure; any minor volume change in the system, including compression and creep of the membrane, can result in a drop in the cell pressure. For this reason, the permeability tests were conducted within 30 min of attainment of the specified cell pressure.

Experimental Results and Analysis

Altogether, 272 permeability tests were conducted on three samples of Indiana Limestone. During testing, the temperature in the laboratory varied between 19°C and 21°C, and the viscosity of the water was estimated to be $\mu \approx 10^{-6}$ kN s/m^2. In the first test (test A), the limestone sample was subjected to loading and partial unloading as shown in Figure 3. Each circle represents the average of three values of the permeability corresponding to each level of the applied cell pressure. Over the cell pressure range of 5 to 60 MPa, permeability tests were conducted at 2.5 MPa intervals at a constant flow rate of 1 mL/min. The upper limit of 60 MPa is a suitable stress level for simulating the self-weight stresses in rock formations up to 2 to 3 km, representative of depths at which underground repositories are constructed in waste management endeavors (Laughton et al. 1986; Chapman and McKinley 1987; Gnirk 1993; Selvadurai and Nguyen 1997). At the start of the initial experiment, the permeability of the limestone sample at a reference confining pressure of 5 MPa was approximately 1.6×10^{-14} m^2. At a confining pressure of 60 MPa, the permeability reduced to approximately 3.9×10^{-15} m^2. This sample also shows a slight increase in the permeability beyond the 50 MPa level. The reasons for this behavior are not entirely clear: it is likely that some form of microcracking may have been initiated as a result of inhomogeneity in the stiffness characteristics of the cylindrical sample. The observed discontinuity is approximately 14% of the range of reduction of the permeability, which is not insignificant but at the same time does not detract from the general trends observed in the test with respect to reduction of permeability with increase of isotropic confining stress. In a second experiment (test B), a separate limestone specimen was subjected to the initial confining pressure of 5 MPa, with a staged increase up to a maximum confining pressure of 60 MPa, in stages of 5 MPa over both the pressurizing and the depressurizing paths. Three permeability tests were conducted at each stress level, and the results are shown in Figure 4. In the final test (test C), a third sample of the limestone was subjected to pressurizing-depressurizing cycles. The sample was first subjected to the reference pressure of 5 MPa and increased to 15 MPa in increments of 5 MPa and depressurized the same way. At each stress level, three permeability measurements were conducted. The procedure was repeated with isotropic pressures increased to 30, 45, and 60 MPa. Figure 5 presents the relevant experimental data,

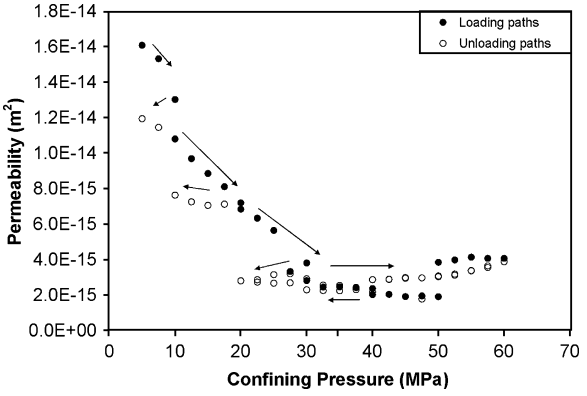

Figure 3. Variation of permeability with isotropic stress history: Loading-partial unloading-reloading (test A).

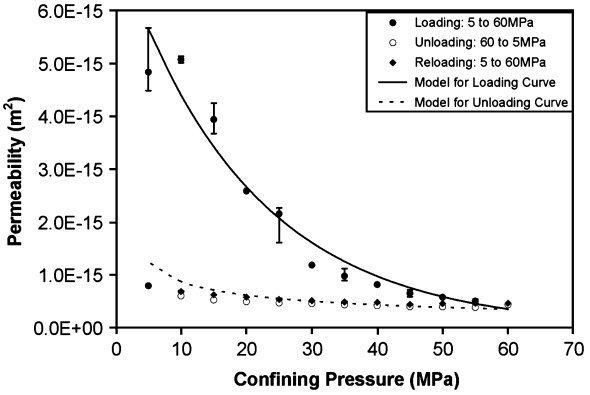

Figure 4. Variation of permeability with isotropic stress history: Monotonic peak loading followed by complete unloading and reloading (test B).

including a second loading sequence up to 60 MPa. Both Figures 4 and 5 indicate the range of values observed in the three tests at each loading increment; the majority of tests showed good repeatability and the range bars are smaller than the symbols used in the figures. At the termination of each series of experiments, the dimensions of the sample were measured; no measurable irreversible deformation was observed in any of the three samples. The experimental data obtained from the three separate experiments were used to develop a preliminary model for describing the evolution of permeability with isotropic stress. The experimental data obtained for the loading and partial unloading (Figure 3) were considered to be too restrictive to model permeability evolution during complete unloading of the limestone. For this reason, the data from the experiments shown in Figure 5 (involving loading, complete unloading, and reloading past the previous maximum value) were used in the development of the model. The modeling describes the permeability evolution with incremental increases in the isotropic confining pressure p, starting from the reference value $p = 5$ MPa up to a maximum of 60 MPa, with unloading to the reference isotropic confining pressure at each stage. By considering the data shown in Figure 5, the permeability evolution during loading, unloading, and reloading can be described by the following approximate relationships:

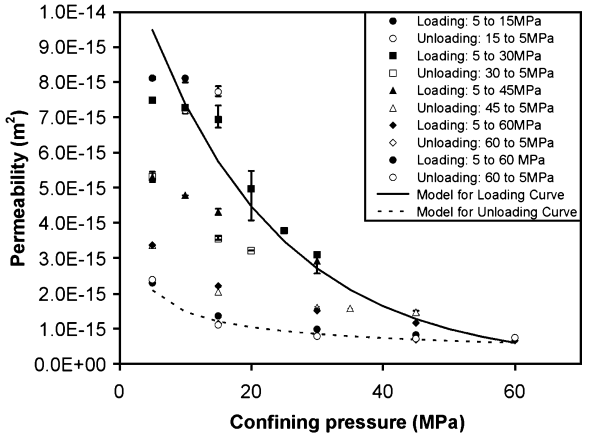

Figure 5. Variation of permeability with isotropic stress history: Monotonic loading and unloading to the reference confining stress state (test C).

1. Loading from reference pressure p_0 to compression p: The permeability evolution $K(p)$ is described by:

$$\frac{K(p)}{K(p_0)} \approx \frac{3}{2}\exp\left(-\frac{p}{4p_0}\right);\ p > p_0;\ dp > 0 \qquad (1)$$

where $K(p_0)$ is the permeability at the reference confining stress p_0.

2. Unloading from p* to $\hat{p}$: The evolution of permeability is described by:

$$\frac{K(p)}{K(p_0)} \approx \frac{3}{2}\exp\left(-\frac{p^*}{4p_0}\right)\sqrt{\frac{p^*}{p}};\ p_0 < \hat{p} < p < p^*;\ dp < 0 \qquad (2)$$

3. Reloading from $\hat{p}$ to $p(< p^*)$: The evolution of permeability is described by:

$$\frac{K(p)}{K(p_0)} \approx \frac{3}{2}\exp\left(-\frac{p^*}{4p_0}\right)\sqrt{\frac{p^*}{p}};\ \hat{p} < p < p^*;\ dp > 0 \qquad (3)$$

4. Reloading past p*: The evolution of permeability is described by:

$$\frac{K(p)}{K(p_0)} \approx \frac{3}{2}\exp\left(-\frac{p}{4p_0}\right);\ p > p^*;\ dp > 0 \qquad (4)$$

The relationships (Equations 1 through 4) are approximate mathematical expressions that describe the evolution of permeability with isotropic confining pressure over a range of loading-unloading histories. (The pressure p in these equations is the absolute value of the pressure acting on the specimen at any stage of the test. The value p^* can be regarded as any arbitrary confining pressure level at which unloading commences. The value of $\hat{p}$ can be regarded as the termination of the unloading sequence.) Comparison between the predictions from the Equations 1 through 4 and the actual experimental data indicate a maximum error of 12% over the range of confining stresses $p \in$ (10, 60) MPa. The solid lines shown in Figures 4 and 5 indicate the predictions using the model for permeability evolution with a monotonic increase in the isotropic confining pressure p. The permeability evolution during the unloading phase depends on the confining stress level at which the unloading is initiated. Considering the unloading path at the peak value of the application of the confining pressure p^*(=60 MPa) (Figure 4), it can be seen that in both the unloading stage and the reloading stage, the actual permeability evolution follows closely the model predictions. It should also be noted that the maximum fluid pressure recorded during initiation of flow through the sample was approximately 1.05 MPa at the lowest permeability in the range 4.4×10^{-16} m^2 and at the confining

pressure of 60 MPa, and on average, the pressure initiating flow was less than 0.5 MPa. The authors conclude that the permeability alterations are relatively uninfluenced by the variations in the effective stress during flow.

Conclusions

Experiments conducted in connection with this research indicate the irreversible reduction in the hydraulic conductivity that accompanies the application of compressive isotropic confining pressure to a sample of Indiana Limestone. The results of a set of experiments involving monotonic increases in the isotropic confining stress, partial unloading, complete unloading, and reloading beyond the past maximum confining stress were used to develop elementary mathematical expressions for describing permeability evolution in the Indiana Limestone under isotropic compression and unloading. Permeability evolution is a stress state and stress path–dependent process. The exact mechanisms that contribute to alterations in permeability with compressive confining pressures are difficult to pinpoint: Permeability reductions in particular could result from void reduction, pore closure, pore throat collapse, and/or pore clogging. The consistent reduction of the permeability with confining pressure in the loading cycle would suggest that there is a gradual pore reduction as opposed to sudden pore collapse or pore clogging as the mechanism contributing to permeability reduction. The presence of permeability hysterisis would suggest that there are irreversible changes to the pore space, in the form of irreversible pore reduction, resulting from changes to the porous fabric, during the compressive pressurization of the specimen. The techniques for determining such micromechanical alterations in the pore space require recourse to advanced experimentation involving X-ray tomography, image processing, and image quantification in terms of pore distribution characterization as a fabric tensorial measure. Such facilities are nonroutine and were unavailable to the researchers. The phenomenological approach adopted here along with extensions of the experimentation to include generalized stress states can provide phenomenological models that are easily implemented in computational approaches to geoenvironmental studies involving ground water movement in geologic media.

Acknowledgments

The work described in this paper was supported in part by the *Max Planck Forschungspreis in the Engineering Sciences* awarded to the first author by the Max Planck Gesellschaft, Berlin, Germany, and through a Natural Sciences and Engineering Research Council of Canada (NSERC) Discovery Grant. The authors are indebted to Dr. David J. Hart and Dr. Frederic Pellet for their valuable constructive comments.

References

Bernaix, J. 1966. New laboratory methods of studying the mechanical properties of rocks. *International Journal of Rock Mechanics and Mining Sciences* 6, no. 1: 43–89.

Brace, W.F., J.B. Walsh, and W.T. Frangos. 1968. Permeability of granite under high pressure. *Journal of Geophysical Research* 73, no. 6: 2225–2236.

Chapman, N.A., and I.G. McKinley. 1987. *The Geological Disposal of Nuclear Waste*. New York: John Wiley and Sons.

Coste, F., A. Bounenni, S. Chanchole, and K. Su. 2001. A method for measuring hydraulic and hydromechanical properties during damage in materials with low permeability, In *Thermohydromechnical Behaviour of Deep Argillaceous Rock*, ed. N. Hoteit, K. Su, M. Tijani, and J.-F. Shao, 109–116. Rotterdam, The Netherlands: A.A. Balkema.

Fatt, I. 1953. The effect of overburden pressure on relative permeability. *Journal of Petroleum Technology* 5, no. 1: 15–16.

Fatt, I., and D.H. Davis. 1952. Reductions in permeability with overburden pressure. *Transactions of the American Institute of Mining Engineers* 195, no. 3: 329.

Gnirk, P. 1993. *OECD/NEA International Stripa Project Overview, Vol. II, Natural Barriers*. Stockholm, Sweden: SKB.

Gray, D.H. 1962. The effect of stress on the directional properties of reservoir rocks. M.S. thesis, Department of Petroleum Engineering, University of California, Berkeley.

Heystee, R., and J.C. Roegiers. 1981. The effect of stress on the primary permeability of rock cores. A facet of hydraulic fracturing. *Canadian Geotechnical Journal* 18, no. 2: 195–204.

ILIA. 1998. *Indiana Limestone Handbook*, 18th ed. Bedford, Indiana: Indiana Limestone Institute of America Inc.

Jaeger, C. 1972. *Rock Mechanics and Engineering*. Cambridge, UK: Cambridge University Press.

Kiyama, T., H. Kita, Y. Ishijima, T. Yanagidani, K. Akoi, and T. Sato. 1996. Permeability in anisotropic granite under hydrostatic compression and triaxial compression including post-failure region. In *Proceedings of the 2nd North American Rock Mechanics Symposium*, ed. M. Aubertin et al., 1643–1650. New York: Taylor and Francis.

Knutson, C.F., and B.F. Bohor. 1963. Reservoir rock behaviour under moderate confining pressure. In *Proceedings of the 5th North American Rock Mechanics Symposium, University of Minnesota*, ed. J.A. Hudson et al., 627–659. New York: Macmillan.

Kranz, R.L., A.D. Frankel, T. Engelder, and C.H. Scholz. 1979. The permeability of whole and jointed Barre granite. *International Journal of Rock Mechanics and Mining Sciences* 16, no. 2: 225–234.

Lama, R.D., and V.S. Vutukuri. 1978. *Handbook on Mechanical Properties of Rocks. Testing Techniques and Results*, vol. 4. Clausthal, Germany: Trans Tech Publications.

Laughton, A.S., L.E.J. Roberts, D. Wilkinson, and D.A. Gray, ed. 1986. The disposal of long-lived and highly radioactive wastes. In *Proceedings of a Royal Society Discussion Meeting*, 5–189. London: Royal Society.

Lion, M., B. Ledésert, F. Skoczylas, P. Recourt, and T. Dubois. 2004a. How does micropetrography help us to understand the permeability and poromechanical behaviour of a rock? *Terra Nova* 16, no. 6: 351–357.

Lion, M., F. Skoczylas, and B. Ledésert. 2004b. Determination of the main hydraulic and poroelastic properties of a limestone from Buorgogne, France. *International Journal of Rock Mechanics and Mining Sciences* 41, no. 6: 915–925.

Londe, P., and F. Sabarly. 1966. Permeability distribution in arch dam as a function of the stress field. In *Proceedings of the 1st Congress of International Society for Rock Mechanics, Lisbon*, 2, 517–521.

McLatchie, A.S., R.A. Hemstock, and J.W. Young. 1958. The effective compressibility of reservoir rock and its effects on permeability. *Journal of Petroleum Technology* 10, no. 1: 49–51.

Selvadurai, A.P.S. 2004. Stationary damage modelling of poroelastic contact. *International Journal of Solids and Structures* 41, no. 8: 2043–2064.

Selvadurai, A.P.S., and P. Carnaffan. 1997. A transient pressure pulse method for the measurement of permeability of a cement grout. *Canadian Journal of Civil Engineering* 24, no. 3: 489–502.

Selvadurai, A.P.S., and T.S. Nguyen. 1997. Scoping analysis of the coupled thermal-hydrological-mechanical behaviour of the rock mass around a nuclear fuel waste repository. *Engineering Geology* 47, no. 4: 379–400.

Selvadurai, A.P.S., M.J. Boulon, and T.S. Nguyen. 2005. The permeability of an intact granite. *Pure and Applied Geophysics* 162, no. 2: 373–407.

Shimada, M. 2000. *Mechanical Behaviour of Rocks Under High Pressure Conditions*. Rotterdam, The Netherlands: A.A. Balkema.

Shiping, L., L. Yushou, L. Yi, W. Zhenye, and Z. Gang. 1994. Permeability-strain equations corresponding to the complete stress-strain path of Yinzhuang Sandstone. *International Journal of Rock Mechanics and Mining Sciences* 31, no. 2: 383–391.

Suri, P., M. Azeemuddin, M. Zaman, A.R. Kukreti, and J.-C. Roegiers. 1997. Stress-dependent permeability measurement using the oscillating pulse technique. *Journal of Petroleum Science and Engineering* 17, no. 3–4: 247–264.

Wright, M., P. Dillon, P. Pavelic, P. Peter, and A. Nefiodovas. 2002. Measurement of 3-D hydraulic conductivity in aquifer cores at in situ effective stress. *Ground Water* 40, no. 5: 509–517.

Wyble, D.O. 1958. Effect of applied pressure on the conductivity, porosity and permeability of sandstones. *Transactions of the American Institute of Mining Engineers* 213, no. 3: 430–432.

Zhu, W., and T.-F. Wong. 1997. Transition from brittle faulting to cataclastic flow: Permeability evolution. *Journal of Geophysical Research* 102, no. B2: 3027–3041.

Zoback, M.D., and J.D. Byerlee. 1975. The effect of microcrack dilatancy on the permeability of Westerly Granite. *Journal of Geophysical Research* 80, no. B3: 752–755.